Vienna, July 8, 2015

Johann Zmeskal
Stefan Meyer Institute for Subatomic Physics
Vienna, Austria
for the K-d collaboration (P57)

To the chairperson and members of the 20th J-PARC Program Advisory Committee for the Nuclear and Particle Physics Experiments at the J-PARC 50 GeV Proton Synchrotron

Report to answer to the questions asked from the 19th J-PARC Program Advisory Committee:

" The TES methodology, however, is not applicable to P57, where the expected X-rays from K-d atom have large natural widths. The PAC asks P57 to update the proposal including a more detailed study of the S/N ratio considering the possible duty factor of the beam. "

K^-d Collaboration - P57

J. Zmeskal[1] (spokesperson), M. Sato[2] (co-spokesperson), S. Ajimura[3], M. Bazzi[4], G. Beer[5], C. Berucci[1], H. Bhang[6], D. Bosnar[7], M. Bragadireanu[8], P. Buehler[1], L. Busso[9,10], M. Cargnelli[1], S. Choi[6], A. Clozza[4], C. Curceanu[4], A. D'uffizi[4], S. Enomoto[11], L. Fabbietti[12], D. Faso[9,10], C. Fiorini[13,14], H. Fujioka[15], F. Ghio[16], R. Golser[17], C. Guaraldo[4], T. Hashimoto[2], R.S. Hayano[18], T. Hiraiwa[3], M. Iio[11], M. Iliescu[4], K. Inoue[19], S. Ishimoto[11], T. Ishiwatari[20], K. Itahashi[2], M. Iwai[11], M. Iwasaki[2,21], S. Kawasaki[19], J. Lachner[17], P. Levi Sandri[4], Y. Ma[2], J. Marton[1], Y. Matsuda[22], Y. Mizoi[23], O. Morra[9], P. Moskal[24], T. Nagae[15], H. Noumi[3], H. Ohnishi[2], S. Okada[2], H. Outa[2], D. Pietreanu[8], K. Piscicchia[4,25], M. Poli Lener[4], A. Romero Vidal[26], Y. Sada[3], A. Sakaguchi[19], F. Sakuma[2], E. Sbardella[4], A. Scordo[4], M. Sekimoto[11], H. Shi[4], M. Silarski[4,24], D. Sirghi[4,8], F. Sirghi[4,8], K. Suzuki[1], S. Suzuki[11], T. Suzuki[18], K. Tanida[6], H. Tatsuno[11], M. Tokuda[21], A. Toyoda[11], I. Tucakovic[4], K. Tsukada[27], O. Vazquez Doce[12], E. Widmann[1], T. Yamaga[19], T. Yamazaki[2,18], Q. Zhang[2]

[1]Stefan Meyer Institute for Subatomic Physics, Vienna, Austria
[2]RIKEN Nishina Center, RIKEN, Wako, Japan
[3]Research Center for Nuclear Physics (RCNP), Osaka University, Osaka, Japan
[4]Laboratori Nazionali di Frascati dell INFN, Frascati, Italy
[5]Department of Physics and Astronomy, University of Victoria, Victoria, Canada
[6]Department of Physics, Seoul National University, Seoul, South Korea
[7]Physics Department, University of Zagreb, Zagreb, Croatia
[8]National Institute of Physics and Nuclear Engineering - IFIN HH, Romania
[9]INFN Sezione di Torino, Torino, Italy
[10]Dipartimento di Fisica Generale, Universita di Torino, Torino, Italy
[11]High Energy Accelerator Research Organization (KEK), Tsukuba, Japan
[12]Excellence Cluster Universe (TUM), Garching, Germany
[13]Politecnico di Milano, Dipartimento di Elettronica, Milano, Italy
[14]INFN Sezione di Milano, Milano, Italy
[15]Department of Physics, Kyoto University, Kyoto, Japan
[16]INFN Sezione di Roma I, Istituto Superiore di Sanit, Roma, Italy
[17]Isotope Research and Nuclear Physics, University of Vienna, Vienna, Austria
[18]Department of Physics, University of Tokyo, Tokyo, Japan
[19]Department of Physics, Osaka University, Osaka, Japan
[20]Department of Physics, University of Vienna, Vienna, Austria
[21]Department of Physics, Tokyo Institute of Technology, Tokyo, Japan
[22]Graduate School of Arts and Sciences, University of Tokyo, Tokyo, Japan
[23]Laboratory of Physics, Osaka Electro-Communication University, Osaka, Japan
[24]Institute of Physics, Jagiellonian University, Cracow, Poland
[25]Museo Storico della Fisica e Centro Studi e Ricerche Enrico Fermi, Roma, Italy
[26]Universidade de Santiago de Compostela, Santiago de Compostela, Spain
[27]Department of Physics, Tohoku University, Sendai, Japan

Introduction

The antikaon-nucleon ($\bar{K}N$) interaction close to threshold provides crucial information on the interplay between spontaneous and explicit chiral symmetry breaking in low-energy QCD. In this context the importance of kaonic deuterium X-ray spectroscopy has been well recognized, but no experimental results have yet been obtained due to the difficulty of the measurement.

We propose to measure the shift and width of the kaonic deuterium 1s state with an accuracy of 60 eV and 140 eV, respectively. These proposed J-PARC results together with the kaonic hydrogen data (KpX at KEK, DEAR and SIDDHARTA at DAΦNE) will then permit the determination of values of both isoisospin I=0 and I=1 antikaon-nucleon scattering lengths and will provide the most stringent constraints on the antikaon-nucleon interaction, promising a breakthrough for this field.

Making use of the existing E15 apparatus at J-PARC upgraded with a recently developed X-ray detector system, and based on the experience gained with a test measurement of kaonic deuterium with SIDDHARTA, we have developed an experimental setup proposed for the kaonic deuterium measurement at J-PARC. Refined Monte Carlo studies have been performed, including the investigation of the background suppression factors with this setup.

With $8\cdot10^9$ delivered kaons (160 kW·weeks) we demonstrate the feasibility to determine the shift and width of the kaonic deuterium atom 1s state with the aimed accuracy: shift = 60 eV and width = 140 eV (for an assumed width of 800 eV).

Proposed experimental method

The proposed experiment will measure the transition X-ray energies to the ground state of kaonic deuterium atoms with recently developed compact SDDs working at low temperature, and an improved active-to-total-area ratio of 0.8:1 (compared to the SIDDHARTA SDD ratio of 0.2:1). These new SDDs will achieve a better time resolution of the order of 50 ns, due to the shorter drift length (smaller area: 8 mm x 8 mm) and the lower working temperature (~ 50 K).

The experiment E570 at KEK *clearly shows the excellent capability of SDDs for X-ray spectroscopy of kaonic atoms in the environment of an accelerator. In addition the fiducial volume cut technique developed at the* ***KpX experiment*** *has proven to be very efficient in suppressing background events originating from the wall. It shall also be applied in the proposed kaonic deuterium X-ray measurement.*

The experimental challenge of the proposed experiment results from the very small kaonic deuterium X-ray yield and the difficulty to perform X-ray spectroscopy in the high radiation environment of an extracted beam. It is therefore crucial to control and improve the signal-to-background ratio for a successful observation of the kaonic deuterium X-rays. There are two types of background sources; synchronous (correlated) and asynchronous (uncorrelated) to the incoming K^-.

- The synchronous background originates from secondary particles generated by the decays and reactions of kaons (kaon absorption in the target gas or in the walls). These background events are suppressed on one hand by a charged particle veto (scintillator tiles just behind the SDDs) and on the other by charged particle tracking, determining the stopping point of the kaon tracks within the target, and defining a fiducial volume, which is 5 mm away from the wall material. Therefore, the excellent tracking capability of the E15 apparatus is essential for the proposed measurement.

- The asynchronous background originates from the kaon production target. This background will be suppressed by an improved timing capability of the SDD itself. Running the SDDs at a temperature below 50 K reduces the drift time to approx. 50 ns (compared to 700 ns SIDDHARTA type SDDs) for the new type of large area SDDs (4 x 2 matrix with a total active area 5.12 cm^2).

Signal-to-noise evaluation

1. Trigger conditions

The trigger definitions are as follows (detector positions are shown in figure 1):

- beam trigger: $\mathrm{BEAM} = \mathrm{T0} \otimes \mathrm{T1} \otimes \overline{\mathrm{T2} \otimes \mathrm{AC}}$
- first level trigger: $\mathrm{Trigger} = \mathrm{BEAM} \otimes \mathrm{CDH}$ (one charged particle)

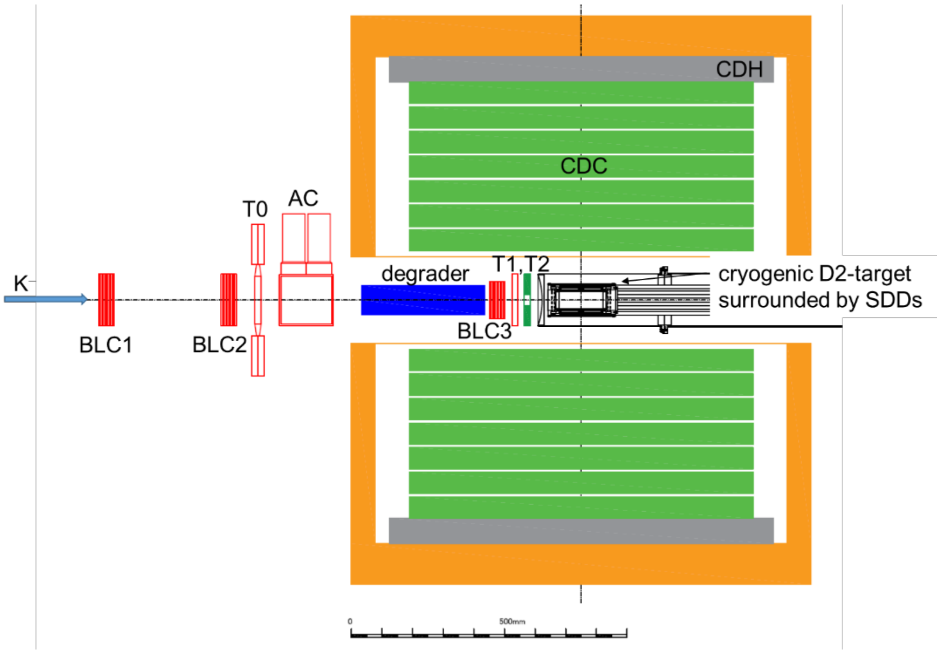

Figure 1: Sketch of the beam defining detectors: The beam line chambers for beam tracking (BLC1, BLC2) are placed after the last beam line magnet D5, followed by the start counter (T0) responsible for the main timing and the silica aerogel Cherenkov counter (AC) for pion discrimination, the energy measurement counter (T1) are placed behind the carbon degrader, a veto counter (T2) and a small vertex beam line drift chamber are placed just in front of the target vacuum chamber. The cylindrical detector hodoscope (CDH) for detecting charged particles (from kaon decay or kaon absorption on the deuteron) surrounds the target cell and the SDD detector system.

The kaon production rate was measured during the beam time of E15 in April 2015 (Run #62) at 24 kW proton beam power, at three kaon momenta 0.9 GeV/c, 1.0 GeV/c and 1.1 Gev/c. The old measurements (Run #29) with kaon momenta from 0.7 GeV/c to 1.0 GeV/c were normalised to the new measured values.

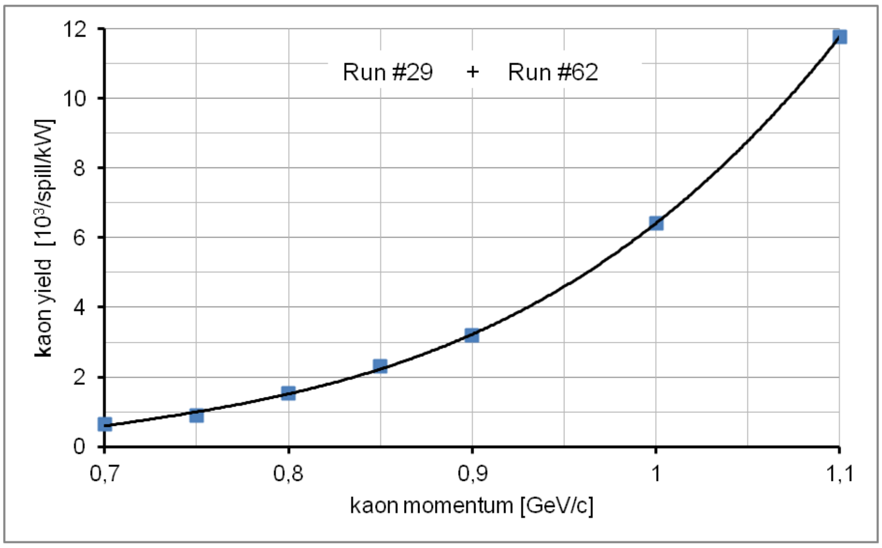

Figure 2: Measured kaon yields from 0.7 GeV/c to 1.1 GeV/c. Data from Run #29 were normalised to Run #62 data (0.9 GeV, 1.0 GeV and 1.1 GeV), measured April 2015.

- kaons produced per spill for a proton beam momentum of 1 GeV/c
  normalised to 1 kW: 6300 kaons/(spill·kW)
  with a K^-/π^- ratio: 0,45 : 1

- kaons produced per spill for a proton beam momentum of 0.7 GeV/c
  normalised to 1 kW: 640 kaons/(spill·kW)
  with a K^-/π^- ratio: 0,05 : 1

In the following MC simulation we use as input a **kaon yield of 640 events per 1 kW and per spill** at a momentum of 0.7 GeV/c (see figure 2).

The beam trigger counter: consists of three plastic scintillators and a silica aerogel Cherenkov counter (see figure 1).

- The T0 counter consists of 5 scintillator bars (material: Saint-Gobain BC420). Each segment has 160 mm (vertical) and 32 mm (horizontal) effective area with a thickness of 10 mm. Two PMTs, HAMAMATSU 6612B, with three-stage boosters are mounted on both ends of each scintillator. The T0 counter is used to determine the main timing of the beam trigger.

- The T1 counter is used for defining the beam and to get a dE/dx measurement just in front of the target chamber. The plastic scintillator (BC420) is 10 mm thick and has a size of 60 mm (vertical) and 60 mm (horizontal), which is just a bit larger than the target cell and is read out by one fine-mesh HAMAMATSU R6152.

- The T2 counter is used as a veto counter, consisting of 4 palstic scintillator segments, arranged such that an area of 120 mm x 120 mm is covered but with a 50 mm hole matched to the diameter of the fiducial volume within the cryogenic target cell (5 mm away from the target walls).

- The aerogel Cherenkov counter (AC), which uses silica aerogel produced by Chiba-University, has an effective area of 180 mm (width) × 100 mm (height) × 10 mm (thickness). Cherenkov photons, which radiate in beam direction are reflected by optical mirrors. The photons are read out by fine-mesh HAMAMATSU R5543 PMs. On-line pion identification is performed with the AC at a threshold level of ~5 photoelectrons, with a pion detection efficiency of 99%.

Expected kaon rates:

beam trigger: BEAM $= T0 \otimes T1 \otimes \overline{T2 \otimes AC}$

per spill and kW	T0	$T0 \otimes T1 \otimes \overline{T2 \otimes AC}$
expected kaon events	640	17
expected pion events	13000	5

first level trigger: Trigger $= BEAM \otimes CDH$

per spill and kW	BEAM	BEAM ⊗ CDH
expected kaon events	17	10
expected pion events	5	0

2. Degrader optimisation

The kaon beam spread determined during the latest run at the K1.8 BR in April 2015 with a kaon momentum of 1000 MeV/c is shown in figure 3. To achieve the maximal value of kaon stops in the gas target we use these measured values as input for the MC simulation in order to optimise the degrader thickness.

For use as a kaon degrader, several materials (carbon, polyethylene and iron) were compared in MC simulations using the GEANT4 package (the low energy electromagnetic processes were simulated using the Livermore model, while the negative kaon absorption at rest was described by a G4 update). The highest stopping density was obtained with a carbon degrader of about 400 mm thickness and kaons with a central momentum of 700 MeV/c.

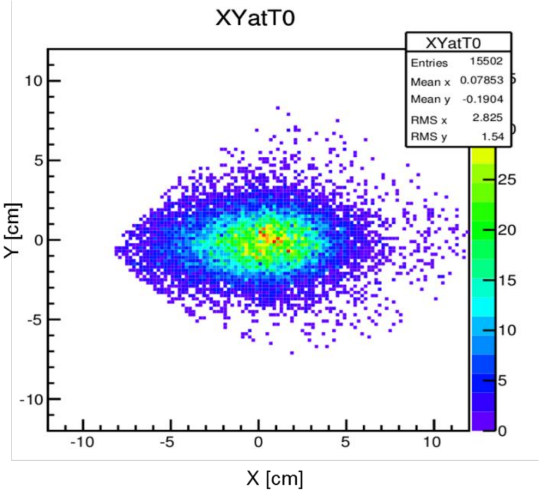

Figure 3: X-Y distribution at the T0 counter position, measured April 2015 during E15 beam time.

In table 1 the optimised results for the carbon degrader thicknesses are summarised for gas and liquid targets.

degrader thickness [cm]	kaon target stops per beam kaon (x10^{-3})	target density
40	0.31	0.03
40	0.60	0.05
39	9.5	1.0

Table 1: Kaon stopping densities in gaseous and liquid targets, optimised for a kaon momentum of 700 MeV/c. The target density is given relative to the liquid deuterium density (LDD).

Figure 4 shows the results of the kaon stopping simulation for a gaseous deuterium target of 5% LDD, with a carbon degrader thickness of 40 cm. The GEANT4 simulation to optimise the kaon stops in deuterium started with 7.10^6 K^- events and a kaon momentum of 0.7 GeV/c at the T0 counter.

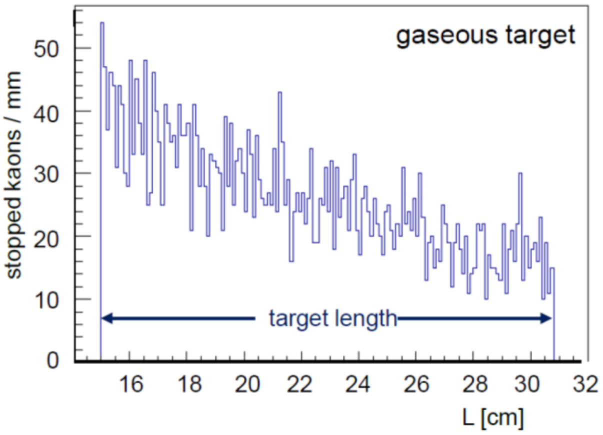

Figure 4: Kaon stopping distribution in the deuterium gas target with a gas density of 5% LDD. Starting with $7\cdot10^6$ kaons before the degrader, $4.2\cdot10^3$ kaons are stopped in the target gas.

3. Synchronous and asynchronous background

Figure 5 shows the correlation between stopped kaon events measured with the kaon monitor and “good” SDD events (above low and below high threshold). The data were taken from the kaonic hydrogen measurement done at DAFNE-LNF with SIDDHARTA.

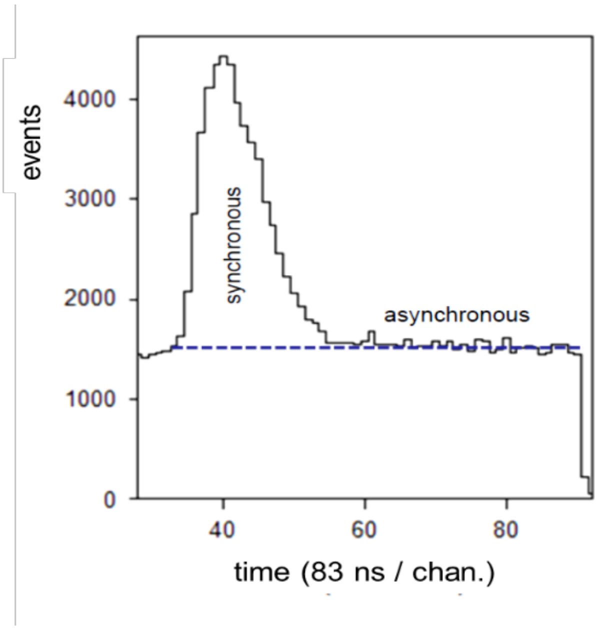

Figure 5: The synchronous background is produced due to kaon absorption on the nucleus or due to emission of X-rays, if a kaonic atom was formed in the materials of the wall.

The synchronous background originates from secondary particles generated by the decays and reactions of kaons (kaon absorption in the target gas or in the walls):
If one of the particles listed in table 2 passes through the active SDDs area, the generated charge is above the upper threshold and an “overflow” event will be recorded. However, under special circumstances (see figure 6) the collected charge falls into the energy region of interest, for example due to a particle passing through the border of the SDD where charge will be deposited and a small portion of which leaks into the active detector area. A charged particle veto (scintillator tiles just behind the SDDs) will reduce this “dangerous” type of background.

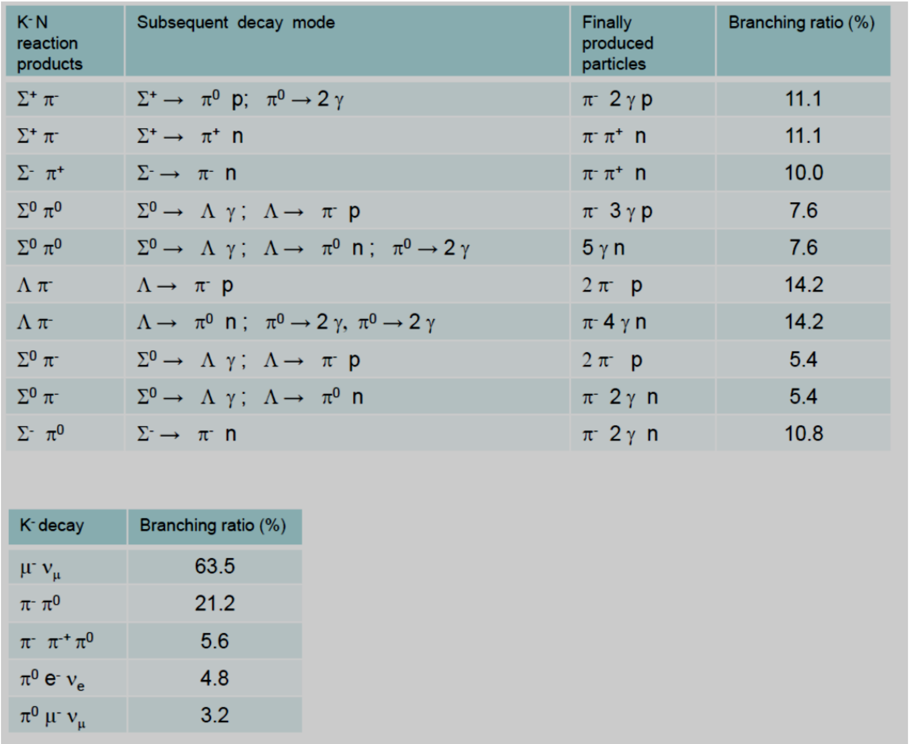

$K^- N$ reaction products	Subsequent decay mode	Finally produced particles	Branching ratio (%)
$\Sigma^+ \pi^-$	$\Sigma^+ \rightarrow \pi^0 p;\ \pi^0 \rightarrow 2\gamma$	$\pi^-\ 2\gamma\, p$	11.1
$\Sigma^+ \pi^-$	$\Sigma^+ \rightarrow \pi^+ n$	$\pi^- \pi^+ n$	11.1
$\Sigma^- \pi^+$	$\Sigma^- \rightarrow \pi^- n$	$\pi^- \pi^+ n$	10.0
$\Sigma^0 \pi^0$	$\Sigma^0 \rightarrow \Lambda \gamma;\ \Lambda \rightarrow \pi^- p$	$\pi^-\ 3\gamma\, p$	7.6
$\Sigma^0 \pi^0$	$\Sigma^0 \rightarrow \Lambda \gamma;\ \Lambda \rightarrow \pi^0 n;\ \pi^0 \rightarrow 2\gamma$	$5\gamma\, n$	7.6
$\Lambda \pi^-$	$\Lambda \rightarrow \pi^- p$	$2\pi^-\ p$	14.2
$\Lambda \pi^-$	$\Lambda \rightarrow \pi^0 n;\ \pi^0 \rightarrow 2\gamma,\ \pi^0 \rightarrow 2\gamma$	$\pi^-\, 4\gamma\, n$	14.2
$\Sigma^0 \pi^-$	$\Sigma^0 \rightarrow \Lambda \gamma;\ \Lambda \rightarrow \pi^- p$	$2\pi^-\ p$	5.4
$\Sigma^0 \pi^-$	$\Sigma^0 \rightarrow \Lambda \gamma;\ \Lambda \rightarrow \pi^0 n$	$\pi^-\ 2\gamma\ n$	5.4
$\Sigma^- \pi^0$	$\Sigma^- \rightarrow \pi^- n$	$\pi^-\ 2\gamma\ n$	10.8

K^- decay	Branching ratio (%)
$\mu^- \nu_\mu$	63.5
$\pi^- \pi^0$	21.2
$\pi^-\ \pi^+ \pi^0$	5.6
$\pi^0 e^- \nu_e$	4.8
$\pi^0 \mu^- \nu_\mu$	3.2

Table 2: Listed kaon nucleon absorption rates and kaon decay channels as used for the MC simulation

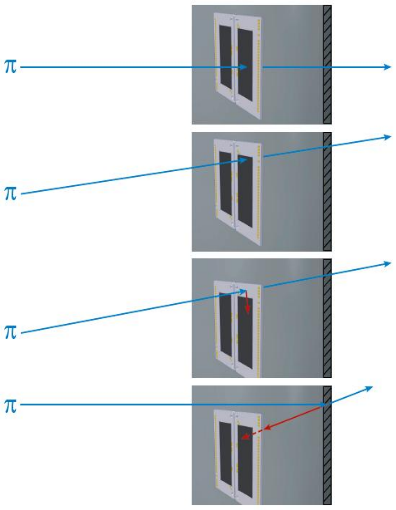

MIP traversing SDD at some distance from the edge → large signal > 150 keV

MIP traversing SDD at the edge of the active area → small signal

electron from secondary produced near the SDD

X-ray or electron from secondary produced in the setup

Figure 6: The sketch shows possible ways a particle might generate

In addition, kaon stops in the target wall or entrance window material will produce kaonic atom X-rays (like kaonic carbon, nitrogen,…. see figure 7). With charged particle tracking, as is available with the E15 apparatus, the determination of the kaon stopping point is possible within the target volume. This method will allow the definition of a fiducial volume within the target (5 mm away from the target wall and entrance window), allowing to the exclusion of wall stops.

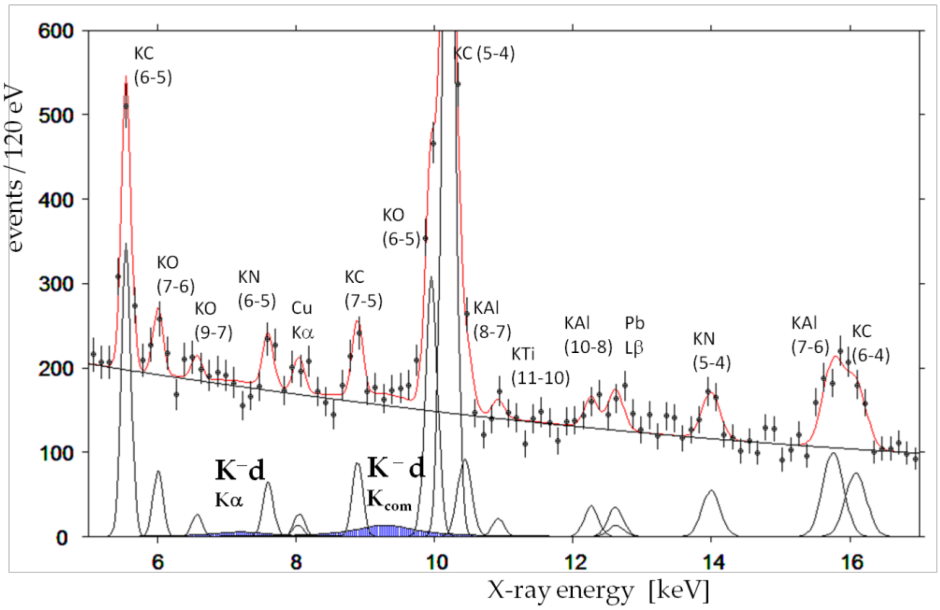

Figure 7: Background measurement performed at LNF with SIDDHARTA (no fiducial volume cut). The region of $K^{-}d$ is indicated in "blue" for a shift of -800 eV and a width of 800 eV.

<u>The asynchronous background</u> originates from the production target. To get an estimate of the background events produced, we use the studies done by the E17 collaboration (see table 3) in their status and run plan report submitted to the 13th PAC (January 2011).

	KEK E570	J-PARC E17
Time Resolution ΔT (ns)	130	220
SDD Efficiency ϵ_{SDD} (%/all SDDs)	0.13	0.95
SDD Single Hit rate F_{SDD} (s^{-1})	105	50
SDD OR / spill	210	100
spill length (s)	2	2
Spill duty factor D_{spill}		0.3
Continuum BG / 50 eV /2000 KHeL_α	25	18 (estimation)
from kaon absorption	14	14 (estimation)
from beam	11	4 (estimation)

Table 3: Comparison of the experimental conditions in KEK E570 and J-PARC E17. Background counts for KEK E570 were evaluated by using timing and energy spectra. Time resolution and SDD OR / spill for J-PARC E17 are measured values during beam commissioning in November 2010.

Using the numbers from table 3 the ratio of asynchronous to synchronous background was estimated to be 4:14, for a SDD drift time window of 220 ns. We expect an improved timing capability using the new SDD in the order of 50 ns, therefore we estimate that the asynchronous background will be approximately 10% of the synchronous one.

4. Geant4 simulation of the K^-d spectrum

For the simulation of the K^-d spectrum, including synchronous and asynchronous events we used the following input:

- simulation starts with $8 \cdot 10^9$ K^- at T0 counter (160 kW·weeks; 80% machine duty factor included)
- total active detector area 246 cm^2
- Kα yield is 10^{-3} for a gaseous target
- shift = – 800 eV and width = 800 eV
- using first level trigger condition
- including fiducial cut and charged particle veto

The final numbers are summarised in table 4, while figure 8 shows the spectrum achieved with a signal-to-noise ratio of 1:3. In total approximately 850 Kα will be collected, which will permit the determination of the shift and width with a precision of 60 eV and 140 eV, respectively. The statistical significance of the Kα-line is ~ 12 σ.

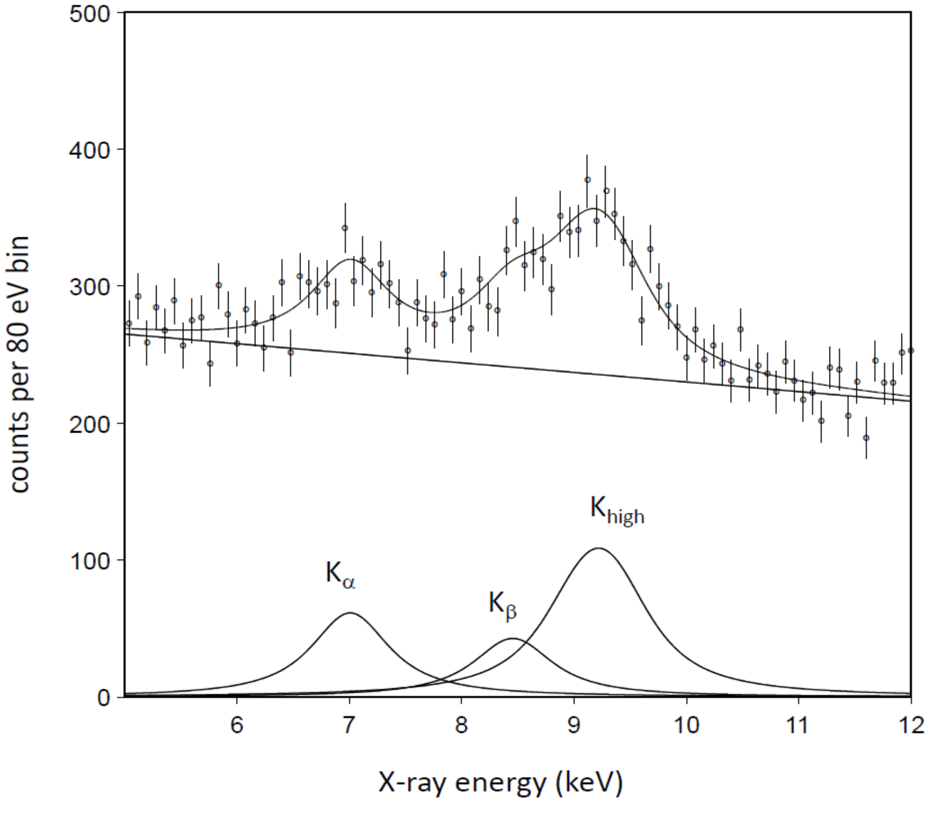

Figure 8: Simulated kaonic deuterium spectrum. The GEANT4 simulation started with $8 \cdot 10^9$ kaons, assuming a shift of -800 eV, a width of 800 eV and an X-ray yield of 0.1%. About 850 Kα events are collected, which leads to a precision of the fit result in this statistical sample: 60 eV (shift) and 130 eV (width).

number of K^- at T0 (per spill and kW)	640
BEAM = $T0 \otimes T1 \otimes \overline{T2 \otimes AC}$	17
BEAM ⊗ CDH (one charged particle)	10
stopped kaons in gaseous deuterium	0.4
total synchronous BG per keV @ 7 keV	$6.0\cdot10^{-2}$
synchronous BG per keV @ 7 keV with fiducial cut and charged particle veto	$1.3\cdot10^{-4}$
asynchronous BG per keV @ 7 keV	$1.3\cdot10^{-5}$
detected Kα events for a yield Y(Kα)=0.1% with fiducial cut and charged particle veto	$5.5\cdot10^{-5}$

Table 4: The evaluation of the background rates and the finally produced Kα events starts with the number of kaons per spill and kW at the beam counter T0. This kaon number, to start with, is extracted from the E15 measurement in April 2015.

Using the final number given in table 4, we calculate for an integrated beam power of 160 kW·weeks (applying a machine duty factor of 80%) a total number of 8.10^9 K^- events on T0, or **850 Kα events** (see figure 8).

With this setup, the final goal will be reached to extract shift and width with the aimed precision of 60 eV and 140 eV, respectively.